Journal of Water Process Engineering 34 (2020) 101148

Contents lists available at ScienceDirect

Journal of Water Process Engineering

journal homepage: www.elsevier.com/locate/jwpe

Resource recovery from an aerobic granular sludge process treating domestic wastewater

Inci Karakas[a], Stanley B. Sam[b], Ender Cetin[a], Ebru Dulekgurgen[b], Gulsum Yilmaz[a,*]

[a] Istanbul University-Cerrahpasa, Faculty of Engineering, Environmental Engineering Department, Avcilar, 34320, Istanbul, Turkey
[b] Istanbul Technical University, Faculty of Civil Engineering, Environmental Engineering Department, Maslak, 34469, Istanbul, Turkey

ARTICLE INFO

Keywords:
Aerobic granular sludge
Irrigation water
Resource recovery
Structural extracellular polymeric substances (EPS)
Polyhydroxyalkanoates (PHAs)

ABSTRACT

This study presents the application of resource recovery from domestic wastewater such as irrigation water, structural extracellular polymeric substances (EPS), and polyhydroxyalkanoates (PHAs). The resource recovery system consisted of an aerobic granular sludge (AGS) reactor processing domestic wastewater and an external membrane reactor receiving the AGS effluent. The AGS effluent contained large numbers of biomass patches detached from the granular sludge. Therefore, the external membrane served to eliminate the biomass patches and individual bacteria from the AGS effluent. The permeate of the membrane reactor was compared with the national irrigation water standards. The results showed that the membrane effluent was suitable to be used as irrigation water, but the boron parameter should be checked for long-term irrigation. Extracellular polysaccharides recovered from the granular sludge were characterized as structural EPS. The analyses showed that PHA accumulating organisms, namely Uncultured *Candidatus Competibacter* sp. and *Competibacteraceae*, were dominant in the AGS reactor, and the PHA content of the AGS was approximately 10 % when operated under high organic loading rate conditions. PHAs, therefore, may also be obtained from AGS. For the management of membrane concentrate and zero-waste discharge approach, it is recommended to investigate the recovery possibilities of structural EPS and PHA biopolymers from the membrane concentrate further because the effluent of AGS contained mostly biomass patches detached from granular sludge.

1. Introduction

The recovery of water, energy, and nutrient resources from municipal wastewater provides a promising solution to a number of prevalent economic, environmental, and social issues [1]. First, water recycling started with desalination processes in the 1970's [2] and was then applied to industrial wastewater [3]. Membrane technology has made water recycling feasible by decreasing the cost. However, the concentrate of the membrane reactor can be a challenge that needs to be managed. Therefore, the membrane concentrate should be carefully managed for recovery purposes by selecting proper pre-treatment units. Nowadays, forward osmosis (FO)-based processes present a novel technology that may simultaneously produce high quality effluents and pre-concentrated wastewater for anaerobic treatment to facilitate the recovery of energy, water, and nutrients. However, issues of salinity accumulation, membrane fouling, and anaerobic treatment integration have not been adequately addressed and limit the practical application of these hybrid systems [1].

In the last decade, wastewater has become a resource rather than a pollutant, and wastewater treatment plants (WWTP) are described as resource recovery systems (RRS) [4]. Researches showed that phosphorus [5], bioplastics [4], biopolymers [6], metals [7], and even cellulose [8] might be recovered from wastewater.

Aerobic granular sludge (AGS) technology has been an innovative technology in wastewater treatment. AGS has numerous advantages such as simultaneous carbon, nitrogen, and phosphorus removal in a single reactor, smaller footprint, and less energy requirement when compared with conventional activated sludge systems [9]. Pronk et al. [10] demonstrated that different types of biopolymers can be extracted from AGS depending on the microbial community cultivated. Recently, sialic acids have been discovered in the extracellular polymeric substances (EPS) of seawater-adapted AGS [11]. A better understanding of the EPS matrix will lead to improved strategies for resource recovery in wastewater treatment systems [12,13].

The cultivation, the micro- and macro-structure, and the long-term operation of two AGS systems fed with high and medium strength domestic wastewater were presented in detail in our previous study [14]. The study highlighted the effects of large concentrations of suspended

* Corresponding author.
E-mail address: gulsum@istanbul.edu.tr (G. Yilmaz).

https://doi.org/10.1016/j.jwpe.2020.101148
Received 4 July 2019; Received in revised form 29 November 2019; Accepted 8 January 2020
Available online 10 February 2020
2214-7144/ © 2020 Elsevier Ltd. All rights reserved.

solids in raw domestic wastewater. The results showed that (a) large concentrations of suspended solids in raw domestic wastewater have a positive effect on granule size and settling properties of the AGS, (b) they can be removed by direct settling inside the reactor and adhesion onto granules, and (c) they affect the detachment of biomass together with high shear force applied in the reactors.

This study focuses on a novel resource recovery approach by which irrigation water, structural EPS, and polyhydroxyalkanoates (PHAs) might be recovered. The resource recovery system consisted of an AGS reactor processing domestic wastewater and an external membrane reactor receiving AGS effluent. The study evaluated the possibilities of recovering the membrane permeate as irrigation water and recovering structural EPS and PHAs from the granular sludge and even biomass in the membrane concentrate.

2. Material and methods

2.1. Wastewater characterization

Wastewater was collected from Istanbul University-Cerrahpasa Campus and originated from the Engineering Faculty, Technical Sciences High School, and the main refectory. Wastewater was collected three times a week and stored at 4 °C before being fed to the first AGS reactor (R1). In addition, raw wastewater taken to another storage tank was settled at least for 2 h to remove all settleable solids and used as feed for the second AGS reactor (R2). Metals mentioned in the national irrigation water standards were analyzed only once if they were lower than the values in the standards. The analyses of boron, iron, and copper were repeated three times. Table 1 includes the detailed characterization of the raw and settled wastewater.

2.2. Reactors

The first unit in the system was an AGS reactor. Two SBRs were operated in parallel: the first one with raw wastewater (R1) and the second one with settled wastewater (R2). The reactors were column type reactors with 28 L of working volume and were operated for 500 days. During the last five months of operation, stable and mature granules were obtained, and the effluents of AGS reactors were separately fed to an external membrane reactor. The membrane reactor was a lab-scale unit with 5 L of working volume. A microfiltration membrane was used as MF005 (Microdyn-Nadir GmbH, Germany).

2.3. Analytical methods

Effluent samples from the AGS reactors were analyzed after filtering through glass fiber filter paper (Millipore AP40) to eliminate the SS content. The following parameters were determined according to the Standard Methods [15]: COD, BOD_5, TKN, TP, NH_4^+-N, NO_2^- -N, PO_4^{3-}-P, SS, VSS, SO_4^{2-}, Cl^-, pH, alkalinity, oil-grease, anionic surface active agents, and fecal coliform. NO_3^--N was determined using a photometric method (Merck kit: 1097130001). The conductivity was measured by a WTW Level 3 conductivity device. The metal ions were analyzed using ICP-MS (Thermo Elemental X Series 2). Particle size distribution was determined using a Malvern Master Sizer 2000 instrument (Malvern Instruments, UK).

2.4. Extraction and characterization of EPS

The EPS in long-term monitoring was extracted using the method proposed by Frølund et al. [16]. The EPS extraction method and the polysaccharide (PS) and protein (PN) analysis are explained in detail in our previous study [14]. Granular biomass samples from the AGS system were also analyzed for structural EPS characterization. Thus, the extracellular polymeric substances, in particular exopolysaccharides (exoPS), were extracted from the sample using Na_2CO_3 and by heating, as previously outlined by Lin et al. [6]. The extract was added to a $CaCl_2$ solution (in 1:1 ratio; w:v) and incubated for a day for completion of crosslinking reactions. Next day, the hydrogel beads were examined by E-SEM (Quanta FEG 250 SEM). For comparison, same treatments were performed for commercially available sodium alginate (A2158, Sigma). FTIR spectroscopy was performed to assess the chemical composition of the extracts (Perkin Elmer Spectrum 100).

Table 1
Detailed characterization of the raw and settled wastewater used in this study.

Parameter	Raw Wastewater	Settled Wastewater	Number of Sample
pH	6.3-7.1	6.3-7.1	200
COD_{tot} (mg L^{-1})	1113 (± 273)	893 (± 175)**	194
COD_{sol} (mg L^{-1})	787 (± 194)	757 (± 185)	194
SS (mg L^{-1})	695 (± 311)	221 (± 66)	200
VSS (mg L^{-1})	587 (± 268)	177 (± 57)	200
NH_4^+-N (mg L^{-1})	53 (± 23)	52 (± 22)	154
TKN (mg L^{-1})	79 (± 31)	70 (± 29)	58
PO_4^{3-}-P (mg L^{-1})	8.1 (± 4.8)	8.0 (± 4.9)	154
TP (mg L^{-1})	12.2 (± 5.5)	10.9 (± 5.8)	58
Oil-Grease (mg L^{-1})	*	281 (± 202)	9
Anionic surface active agents (mg LAS L^{-1})	*	2.5 (± 1.5)	8
Mean Size of SS (μm)	220(± 135)	60 (± 40)	21
SO_4^{2-}(mg L^{-1})	*	39 (± 12)	3
Cl^-(mg L^{-1})	*	168 (± 26)	3
Conductivity (μS cm^{-1})	*	1475 (± 176)	3
Ag (mg L^{-1})	*	0.0085	1
Al (mg L^{-1})	*	0.21	1
As (mg L^{-1})	*	0.0098	1
B (mg L^{-1})	*	8.2 (± 1.8)	3
Be (mg L^{-1})	*	0.00092	1
Cd (mg L^{-1})	*	0.015	1
Cr (mg L^{-1})	*	0.068	1
Co (mg L^{-1})	*	0.0024	1
Cu (mg L^{-1})	*	2.4 (± 3.2)	3
Fe (mg L^{-1})	*	0.08 (± 0.11)	3
Hg (mg L^{-1})	*	0.029	1
Pb (mg L^{-1})	*	0.023	1
Li (mg L^{-1})	*	0.0067	1
Mn (mg L^{-1})	*	0.098	1
Mo (mg L^{-1})	*	0.012	1
Ni (mg L^{-1})	*	0.216	1
Se (mg L^{-1})	*	0.024	1
V (mg L^{-1})	*	0.007	1
Zn (mg L^{-1})	*	0.092	1

*not analysed.
**standard deviation.

2.5. PHA analysis

PHAs accumulated in the biomass were determined using gas chromatography (GC). Approximately 10−15 mg of lyophilized biomass was added to a vial. Next, 2 mL of methanolysis solution and 2 mL of chloroform were added. The vial was capped and sealed using parafilm. It was heated using heater block at 100 °C for 140 min [17]. The vials were left to cool down to room temperature after heating. One microliter of deionized water was added into the vial and vortexed for about 30 s. Three layers formed in the vial and the bottom layer was pipetted out into a vial containing a small amount of sodium sulfate (Na_2SO_4). The vial was stirred until a clear solution was obtained. The clear solution was transferred into a GC vial for quantification. GC equipped with an auto-injector was used to analyze the solution. One microliter of the solution was injected into the column fitted to the GC. The specification of GC column and settings are given in Table S1. The samples were calibrated with standard curves prepared using P(3-HB-co-3-HV) (Sigma Aldrich).

2.6. Microscopic examination and microbial community analyses

Mixed liquor samples were collected from R1 (end of aerobic phase) to visually verify the presence of PHB-accumulating organisms and confirm intracellular C-storage in the form of lipid-like inclusions, mainly as PHB. Thin smears were prepared from mixed liquor and smashed AGS granules for PHB-staining. Samples were treated first with Sudan Black B (staining PHB) and then with Safranin O (counter-staining), according to the manual by Jenkins et al. [18]. Microscopic examination of the samples was carried out using a light microscope (Olympus BX60) equipped with a CCD-camera (KameramGen3).

Next generation sequencing (NGS)–based metagenomics were carried out to determine the microbial community. The protocol includes the primer pair sequences for V3 and V4 regions of the 16S rRNA that create a single amplicon of approximately 460 bp [19]. The sequences were classified using Bayesian classifier implanted in mother. The reference and taxonomy files were adopted from the Greengenes database [20]. After the operational taxonomic units (OTUs) were selected and their taxonomic assignment was performed using the SILVA rDNA database, the OTUs were binned into phylotypes [14].

3. Results and discussion

3.1. Performance of AGS reactors

The cultivation, structure, and long-term stability of AGS fed with real domestic wastewater with high and medium concentration of suspended solids were investigated in our previous study [14]. The AGS reactors were operated for 500 days, and operation in the last five months was considered as the stable period (between Day 350 and 500). The studies for recovery of irrigation water and biopolymers from the systems were carried out during the stable period. The effluent concentrations of COD, NH_4^+-N, and PO_4^{3-}-P and removal efficiencies during the stable period are illustrated in Fig. 1 and summarized in Table S2. COD removal efficiencies in both reactors were quite stable and identical (89 % ± 5) in this period, and the corresponding effluent COD values from R1 and R2 were 98 ± 71 mg L^{-1} and 86 ± 38 mg L^{-1}, respectively. The removal efficiencies of NH_4^+-N and PO_4^{3-}-P in both reactors fluctuated unlike the COD removal efficiencies during the stable period because the influent concentrations of NH_4^+-N and PO_4^{3-}-P changed from 20 to 135 mg L^{-1} and from 3 to 21 mg L^{-1}, respectively. The total nitrogen (TN) removal efficiency in both reactors was 70 % ± 16 on an average, and NO_x-N production was negligible at the end of each cycle. The removal efficiency of TP was 75 % ± 13 in R1 and 78 % ± 20 in R2. The removal efficiencies of NH_4^+-N and PO_4^{3-}-P were lower than those of TN and TP because of the hydrolysis of suspended solids (proteins and organic phosphorus) (Fig. 1c–e, and f and Table S2).

The cycle studies were performed weekly for both reactors, and the results of a typical cycle study on Day 429 are given in Fig. 2. The profiles of COD, NH_4^+-N, and PO_4^{3-}-P in a cycle were considerably similar in both reactors. At the end of the anaerobic period, the concentrations increased because of wastewater feeding. All three parameters had increasing trends during the first 60 min of the cycle because the reactors were fed continuously during that period under anaerobic conditions. Hydrolyses of particulate matter, causing an increase in soluble COD, and adsorption and/or biochemical conversion by microorganisms, resulting in a decrease in COD, were the governing bio-reactions during the anaerobic phase. The net result of these processes was that the COD concentrations at the end of the anaerobic period in both reactors were 30–40 % lower than the calculated values, denoting that 30–40% of the COD was removed from the bulk liquid by microorganisms. Microbial community analyses showed that Uncultured *Candidatus Competibacter* sp. were the most dominated species in R1 (35 %) and in R2 (8.7 %) during the stable period (Table S3). Additionally, *Accumulibacter* in both reactors was 4–5 % of the total bacteria. The presence of these bacteria may explain the lower COD and the slightly higher PO_4^{3-}-P values obtained by the end of the anaerobic period in comparison to the calculated values. Slightly increased NH_4^+-N concentrations compared to the calculated values at the end of the anaerobic period were attributed to the hydrolysis of particulate matter (proteins). The COD, NH_4^+-N, and PO_4^{3-}-P were removed at the same rate in the following aerobic phase because the main reaction was biological growth. Nitrification was negligible with almost no NO_x-N production during the aerobic phase. Conventional nutrient removal processes (nitrification-denitrification and EBPR) could not be achieved because the conventional nutrient-removing organisms (autotrophic *Nitrosomonas* and *Nitrospira* and heterotrophic phosphate-accumulating *Accumulibacter*) did not get enriched in the AGS reactors [14].

3.2. Water recovery for irrigation purposes

The effluents of AGS reactors had a high SS content due to the short settling time and high shear forces applied in the reactors. An external membrane reactor (MR) was used to eliminate the effluent SS and recover the treated water for irrigation purposes. The effluents of AGS reactors were subjected to treatability studies in the MR thrice. Table 2 presents results of one of those treatability studies conducted on Day 457. The MR was effective in eliminating SS and fecal coliform, whereas no significant improvement was observed in COD, NH_4^+-N, and PO_4^{3-}-P removal efficiencies because a microfiltration membrane was used in the MR system.

The quality of the permeate from the MR was evaluated in comparison to the national irrigation water standards [41]. The effluent of MR in R2 was only analyzed because the parameters analyzed in the MR effluents of both reactors were in the similar range except for COD and NH_4^+-N (Table 2). The results are shown in Table 3. The effluent of the AGS-MR system in R2 was classified as class A in terms of pH, BOD_5, SS, and fecal coliform parameters. It should be noted that the removal efficiency of COD (BOD_5) in both AGS reactors was variable during the study. Therefore, this parameter should be checked for irrigation purposes. The chemical quality of the effluent was also evaluated for degree of restriction on irrigation use (Table 3). II. Class irrigation water was provided because of the evaluation of electro conductivity (EC), total dissolved solids (TDS), sodium adsorption rate (SAR), Na (sprinkler irrigation only), and Cl^- parameters. Boron parameters were found to be quite high in both settled and treated wastewater. Classification of irrigation water by resistance of plants to boron mineral is given in Table S4. According to Table S4, boron-resistant plants such as sugar beet, alfalfa, broad bean, onion, lettuce, and carrot can be irrigated. It was thought that the high concentration of boron may result from detergents used for cleaning. Boron-containing cleaning products are marketed as environmentally friendly products. However, this study emphasizes that the boron parameters should be carefully checked if the treated wastewater is to be recovered as irrigation water and that the use of boron should be managed for future recovery of the treated wastewater.

Heavy metals and toxic element concentrations in the settled wastewater were analyzed and compared with the permissible concentrations at the national agricultural irrigation water standard [41] (Table 4). Most of the heavy metals and toxic element concentrations in the settled wastewater were lower than that of the standard. However, the copper concentration was determined to be higher than the permissible concentration. Therefore, the copper concentration in the effluent of the AGS-MR system was measured and found to be 0.018 mg L^{-1}, which was lower than that of the standard.

Thirty percent of the feeding volume of MR was retained as a concentrate after membrane treatment. As mentioned in the previous study [14], the suspended solids of the AGS reactor effluent consisted of biomass patches detached from the granular sludge. Analyses of EPS showed that the concentration of EPS_{PS} in the concentrate was in a similar range with the concentration of EPS_{PS} in the reactors (Table 2).

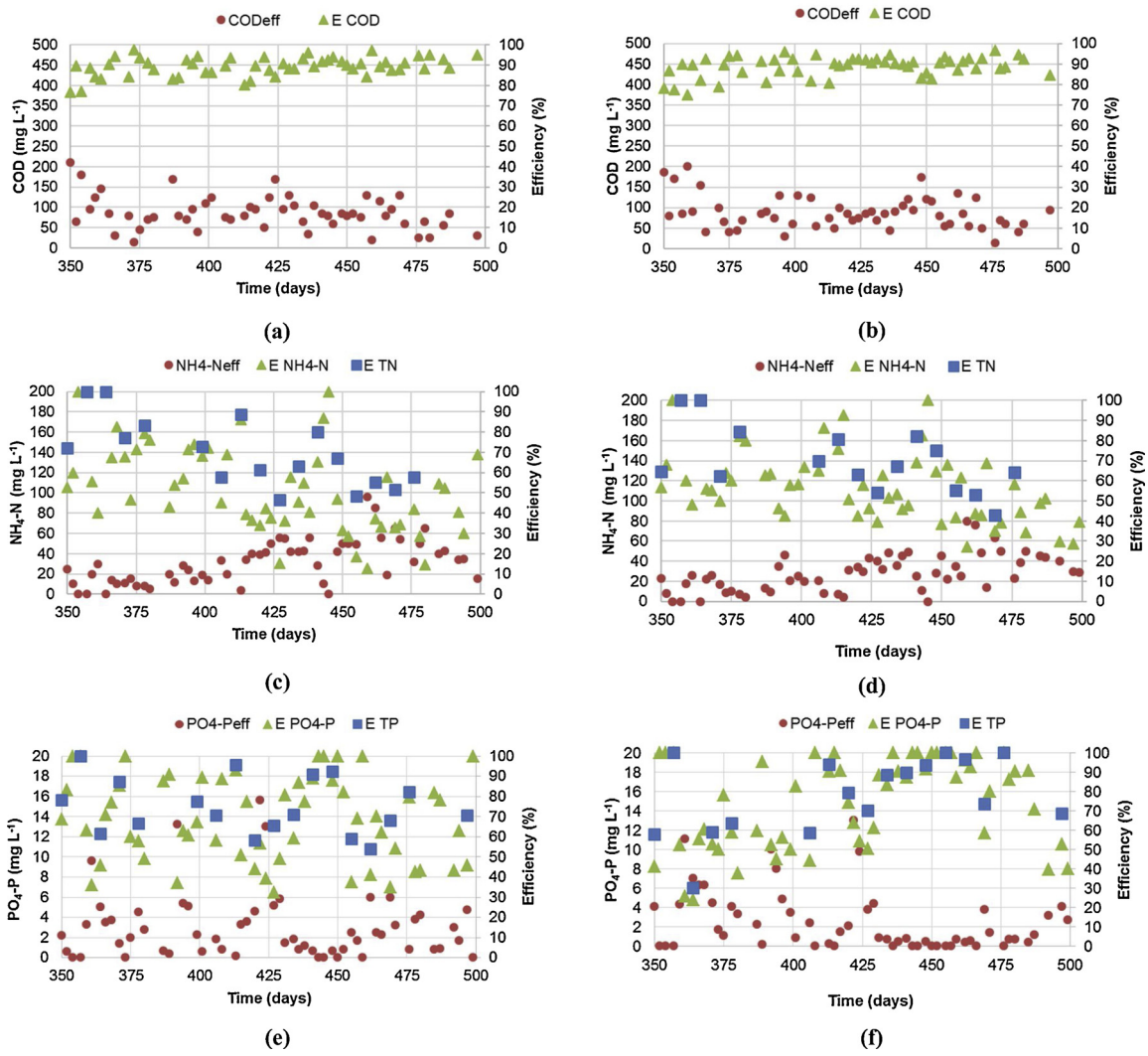


Fig. 1. Effluent concentrations and removal efficiencies of COD, NH_4^+-N, and PO_4^{3-}-P during the stable period in (a), (c) and (e) R1; (b), (d) and (f) R2.

Pishgar et al. [21] demonstrated that noteworthy similarity was observed between the relative abundances of genera enriched in the AGS sample and discharged from the reactor. Therefore, the resource recovery possibilities were evaluated in the biomass of the reactors.

3.3. AGS-related biopolymers and their potential technical usage

3.3.1. Structural EPS of AGS

Extracellular polysaccharides (exoPS) extracted from the granular sludge of the pilot-scale AGS system (R1 fed with raw wastewater) demonstrated gel-forming capacity with divalent cations similar to alginates: a combination of 2 % AGS-exoPS in 2 % $CaCl_2$ produced hydrogel beads, as can be seen in Fig. 3. E-SEM analysis revealed further similarities in terms of the structure and appearance of the hydrogels formed by sodium alginate (Fig. 3c) and the AGS-exoPS (Fig. 3d). Similar results were obtained with the exoPS extract from the granular sludge fed with settled wastewater (R2). Successful ionic hydrogel formation of the exoPS extracted from the granular sludge was in agreement with the results reported by Lin et al. [6] and, Sam and Dulekgurgen [22]Felz et al. [23], and further provides clues of why AGS systems perform better than conventional floccular activated sludge (AS) systems in terms of biomass aggregation, compaction, and

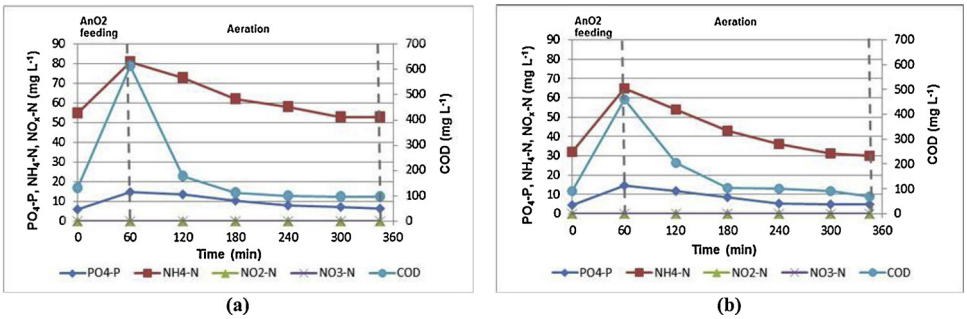


Fig. 2. A typical cycle study on Day 429 in.(a) R1 and (b) R2.

Table 2
Results of the treatability study for irrigation purposes in R1 and R2 (Day 457).

Parameter	R1: Raw WW				R2: Settled WW			
	Influent AGS	Effluent AGS	Effluent MR	AGS Reactor/ Concentrate	Influent AGS	Effluent AGS	Effluent MR	AGS Reactor/ Concentrate
COD (mg L^{-1})	1190	130	120	–	945	55	50	–
NH_4^+-N (mg L^{-1})	73	72	68	–	65	25	25	–
PO_4^{3-}-P (mg L^{-1})	5.5	0	0	–	5.3	0	0	–
SS (mg L^{-1})	1220	820	0	9640/1060	170	140	0	8910/320
$SO_4^=$ (mg L^{-1})	160	33	32	–	48	41	32	–
Cl^-(mg L^{-1})	155	150	135	–	150	150	130	–
EC (µS cm^{-1})	1422	1400	1265	–	1350	1245	1079	–
pH	6.46	8.18	–	–	6.46	8.21	–	–
EPS_{PN} (mg BSA gVSS $^{-1}$)	–	–	–	6.6/7.1	–	–	–	5.1/8.1
EPS_{PS} (mg alginate $gVSS^{-1}$)	–	–	–	300/335	–	–	–	270/308
Alkalinity (mg $CaCO_3$ L^{-1})	–	–	350	–	–	–	150	–
Fecal coliform (MPN 100 m L^{-1})	–	–	0	–	–	–	0	–
Volume (L)	–	5	3.5	-/1.5	–	5	3.5	-/1.5

settling. Felz et al. [23] employed various extraction methods to isolate EPS from aerobic granular sludge samples, and used the ionic hydrogel (cross-linked through Ca^{+2} ions) formation test to determine whether the extracted EPS were structural polymers supporting granulation by contributing to gel formation. They reported that among all extracts they tested, only the EPS extracted by the Na_2CO_3 and heating procedure and the exoPS fraction of that isolated by additional steps (referred as ALE-extraction) formed stable ionic hydrogel beads, thus considered as the structural EPS of the AGS. Accordingly, the exoPS extracted in this study from the AGS of the pilot-plant was addressed as the structural EPS contributing to the granular structure of the biomass, which displayed excellent settling properties in the compact treatment system.

Results of the FTIR spectroscopy are visually presented in Fig. 4 and comparatively summarized in Table 5. The strong broad bands detected at $3600-3000\ cm^{-1}$ region and the weaker ones at around $2900\ cm^{-1}$ were assigned to O—H and C—H stretching vibrations, respectively, associated with hydrocarbons. Between 1700 and 1200 cm^{-1} region, mainly associated with the presence of proteins, the spectra of sodium alginate and the structural EPS were different: spectra of the structural EPS displayed peaks at $1700-1600\ cm^{-1}$ (amide-I), $1600-1500\ cm^{-1}$ (amide-II), and $1300-1200\ cm^{-1}$ (amide-III) regions: for the AGS-EPS from R1 and R2, respectively, peaks at 1627 and 1628 cm^{-1} were attributed to C═O stretching vibrations associated with proteins (amide-I region). Those detected at 1540 and 1532 cm^{-1} were attributed to N—H bending and C—N stretching vibrations in —CO—NH of proteins (amide-II region). The peaks at the amide-III region were weaker than those at the amide-I and amide-II regions. They were at 1237 and 1228 cm^{-1} and attributed to the C—N stretching vibrations in proteins. Those peaks might be considered as implying the presence of some proteins in the structural EPS of AGS from R1 and R2, even though the extraction procedure applied in this study was same/similar to those proposed for extraction of ALE from AGS ([6,23], respectively). Alternatively, they might be associated with some other functional groups, as also reported by some researchers. In their study on characterization of EPS extracted from a soil-isolate and relation between the EPS composition and bioflocculation capacity, Yuan et al. suggested that some of the stretches at the amide-I, II, III regions attributed to proteins were possible with amino-sugars and N-acetylated derivatives [24]. Badireddy et al. [25] conducted a study to characterize the EPS from AS and to determine the role of different EPS components on aggregation. They interpreted the

Table 3
Comparison of treated wastewater by AGS-MR system with national agricultural irrigation water standards [41].

Parameter	AGS-MR system	Recovered Water Quality for Irrigation		Classification of treated wastewater for degree of restriction on irrigation use		
		Class A	Class B	None I. Class	Moderate II. Class	Severe III. Class
pH	8.21	6–9	6–9			
BOD_5 (mg L^{-1})	15	< 20	< 30			
SS (mg L^{-1})	0	< 5	< 30			
Fecal Coliform (MPN 100 m L^{-1})	0	0	< 200			
EC (µS cm^{-1})	1079			< 700	700–3000	> 3000
TDS (mg L^{-1})	691			< 500	500–2000	> 2000
SARadj*						
0-3				EC≥ 0.7	0.7–0.2	< 0.2
3-6	4.03			EC≥ 1.2	1.2–0.3	< 0.3
6-12				EC≥ 1.9	1.9–0.5	< 0.5
12-20				EC≥ 2.9	2.9–1.3	< 1.3
20-40				EC≥ 5.0	5.0–2.9	< 2.9
Na (mg L^{-1})						
Surface irrigation				< 3	3–9	> 9
Sprinkler irrigation	119			< 70	> 70	
Cl- (mg L^{-1})						
Surface irrigation	130			< 140	140–350	> 350
Sprinkler irrigation				< 100	> 100	
Boron (mg L^{-1})	6.07			< 0.7	0.7–3.0	> 3.0

*SAR value was used instead of SAR_{adj}.

Table 4
Comparison of heavy metals and toxic element concentrations in wastewater with national agricultural irrigation water standard [41].

Parameter (mg L^{-1})	Settled Wastewater	Permissible heavy metals and toxic elements concentrations	
		Long term irrigation for all types of soil	Short term irrigation (< 24 years) for clayey soil at pH 6.0–8.5
Aluminium	0.21	5.0	20.0
Arsenic	0.0098	0.1	2.0
Beryllium	0.00092	0.1	0.5
Boron	6.9	–	2
Cadmium	0.01	0.01	0.05
Chrome	0.068	0.1	1.0
Cobalt	0.0024	0.05	5.0
Copper	4.7	0.2	5.0
Fluoride	*	1.0	15.0
Iron	0.0052	5.0	20.0
Lead	0.023	5.0	10.0
Lithium	0.0067	2.5	2.5
Manganese	0.098	0.2	10.0
Molybdenum	0.01	0.01	0.05
Nickel	0.2	0.2	2.0
Selenium	0.02	0.02	0.02
Vanadium	0.007	0.1	1.0
Zinc	0.092	2.0	10.0

*not analysed.

FTIR bands at 1740 − 1720 cm^{-1} and 1270 − 1230 cm^{-1} as implying the presence of O-acetylated carbohydrates, which have been suggested to take part in cell aggregation, adhesion, and biofilm integrity. Lin et al. [6], who evaluated the FTIR spectra of their AGS and its ALE, assigned the peaks at 1240 cm^{-1} to the presence of O-acetyl ester for bacterial alginates.

The region at 1500 − 1300 cm^{-1} is referred as housing the carboxylic group containing- and hydrocarbon-like compounds. Accordingly, peaks at 1444 and 1452 cm^{-1} in the spectra of extracts from R1 and R2, respectively, were assigned as the C—H bending (methylene group) and those at 1404 and 1398 cm^{-1} as the C═O symmetrical stretching of $-COO^-$ groups. In particular, Badireddy et al. [25] suggested that the peak at around a similar position (1398 cm^{-1}) was due to the υ_s COO^- of carboxylate group attributed to uronic acids. Weak peaks at 1314 and 1312 cm^{-1} might be due to the C—H stretching associated with lipids [24,25].

The region at 1200 − 900 cm^{-1} is associated with the polysaccharides and nucleic acids. The strong peak at 1027 cm^{-1} recorded for sodium alginate, as well as the medium broad peaks at 1036 and 1055 cm^{-1} observed for the extracts of R1 and R2, respectively, were assigned to the C—O—C ring vibrations and the C—OH stretches of the polysaccharides in those samples. In particular, Leal et al. [26] and Pronk et al. [10] addressed the peaks they detected within the 1150 − 950 cm^{-1} region as being associated with the stretching vibrations of pyranose rings.

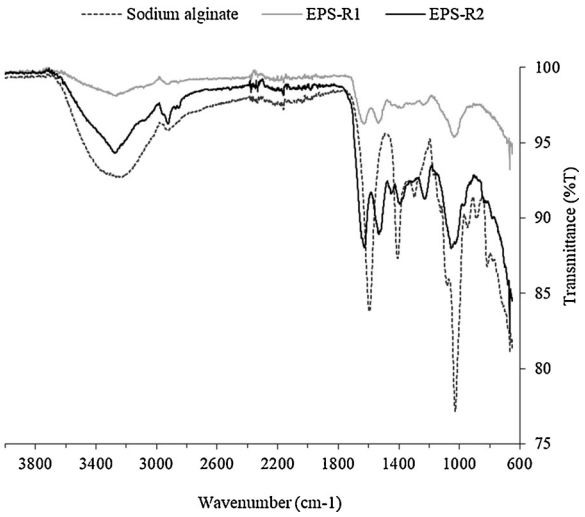


Fig. 4. FTIR spectra of sodium alginate and AGS-EPS from R1 and R2 (fed with raw- and settled wastewater, respectively).

The 900 − 650 cm^{-1} region is referred as the fingerprint region. For sodium alginate, the apparent peaks at 947, 886, and 815 cm^{-1} were assigned to the C—O stretching vibration of uronic acid residues, C1-H deformation of mannuronic acid residues, and the characteristic peak of mannuronic acid residues, respectively, according to the data reported by Leal et al. [26], who employed chemical characterization of the alginic acids extracted from brown seaweeds. They also reported peaks at 902 and 823 cm^{-1} in the secondary derivative spectrum attributed to the C1-H deformation of α-L-guluronic acid residues and deformation vibration of β-D-mannopyranuronic acid residues, respectively. Lin et al. [6] reported same/similar results for the AGS-exoPS which they characterized as ALE. Sam and Dulekgurgen [22] reported peaks at 902 and 879 cm^{-1} at the corresponding fingerprint region, for the extract obtained from an AGS treating brewery wastewater. For the AGS-EPS extracted from R1 and R2 in this study, significantly small yet detectable peaks at the fingerprint region were recorded at 915, 895 cm^{-1} for the AGS-EPS from R1 and at 972, 937/920, 895/838 cm^{-1} for the AGS-EPS from R2, which were different than those reported previously for alginates/ALE. Therefore, it was not possible to directly consider those peaks as indicting the presence of uronic acid residues characteristic of alginates/ALE. Moreover, different findings were also reported in some other studies. For instance, in a study on characterization of EPS derived from an AGS dominated by *Defluviicoccus* sp., the peaks at 929 and 847 cm^{-1} were addressed as referring to the α-linkage between monomers, and the researchers concluded that the AGS-EPS was not ALE, but a different acid soluble structural EPS containing both glucose and galactose as monomers [10]. In some other studies where FTIR spectroscopy was used as one of the techniques for characterization of EPS isolated from different sources, e.g., from floccular AS fed with protein-rich influents [27], from AS dominated by ammonia-oxidizing

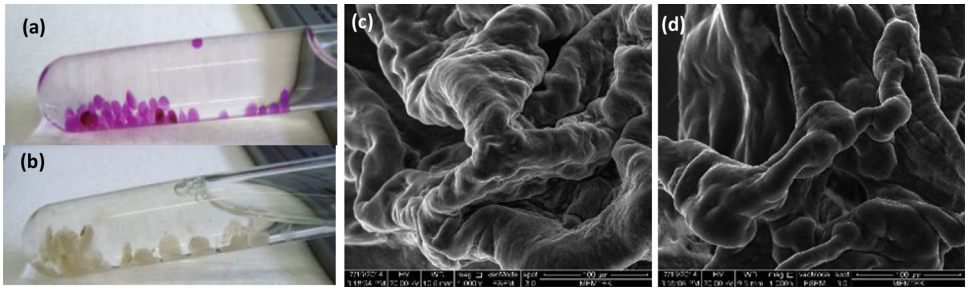


Fig. 3. Gel formation in CaCl2 solution: (a) sodium alginate, (b) AGS-exoPS (R1-raw ww). E-SEM images of hydrogels: (c) sodium alginate, (d) AGS-exoPS. *Note: the pink-color (a) is due to staining with ruthenium red.*

Table 5
Band assignments for FTIR spectra of sodium alginate and the structural EPS extracted from the AGS of R1 and R2 (fed with raw- and settled wastewater, respectively). Data interpretation is based on selected studies including chemical characterization of EPS isolated from various sources.

Wavenumbers (cm^{-1}) / Region	Band position (cm^{-1})			Band assignment
	Alginate	EPS R1	EPS R2	
Hydrocarbons	3600–3000	3600–3000	3600–3000	O–H stretching vibrations associated with hydrocarbons
Hydrocarbons	2928	2920	2926	C–H stretching vibrations associated with hydrocarbons
1700 – 1600 cm^{-1}		1627	1628	C=O stretching associated with proteins
Proteins-amide I				
	1594	–	–	
1600 – 1500 cm^{-1}		1540	1532	N–H bending and C–N stretching vibrations in –CO–NH of proteins
Proteins-amide II				
1500 – 1300 cm^{-1}	–	1444	1452	C–H bending (methylene group)
Carboxylic group containing and hydrocarbon-like compounds	1408	1404	1398	C=O symmetrical stretching of $-COO^-$ grps
	1297	1314	1312	C–H stretching associated with lipids
1300 – 1200 cm^{-1}	–	1237	1228	C–N stretching vibrations in proteins
Proteins-amide III				
1200 – 900 cm^{-1}	1027	1036	1055	C–O–C ring vibrations and C–OH stretches of polysaccharides
Polysaccharides and nucleic acids				
900 – 650 cm^{-1}	947			C–O stretching vibration of uronic acid residues
Fingerprint region	886			C1–H deformation of mannuronic acid residues
	815			Characteristic of mannuronic acid residues
		–	972/965	*Please refer to the text for interpretations*
		915	927/920	
		895	895/838	

bacteria [28], from floccular AS of a full-scale WWTP designed for N-removal [25], the peaks detected at 1000 – 950 cm^{-1} were attributed to the O–P–O stretching associated with nucleic acids, and those at 900 – 600 cm^{-1} region were considered as associated with the ring vibrations from aromatic amino acids and nucleotides.

The FTIR analyses employed in this study showed that the structural EPS of AGS consisted of polysaccharides and possibly some proteins, as revealed by the apparent peaks at the 1200 – 900 cm^{-1} region, and those in the amide I, II, and III regions (Fig. 4). However, it was not possible to resolve the organic functional groups at the fingerprint region, and thus the extracts might not be addressed directly as ALE, despite of some similarities with sodium alginate in that region. Studies on characterization of structural EPS form different AGS systems have shown that a range of different extracellular biopolymers are produced by AGS: as mentioned above, the exoPS extracted from an AGS system treating municipal wastewater displayed chemical and functional similarities with alginates and therefore addressed as ALE [6]; the EPS extracted from an AGS dominated by *Defluviicoccus* sp. was characterized as an acid soluble structural EPS different than ALE [10]; the EPS extracted from a seawater-adapted AGS was determined to include sialic acids, in particular as the terminal sugar residues of glycoproteins [11]; another AGS-EPS was shown to include hyaluronic acid-like and sulphated glycosaminoglycans-like polymers [29].

Apparently, FTIR analyses applied in this study was limited for detailed characterization of the structural EPS extracted from the AGS, and further analyses (i.e., NMR, Raman spectroscopy, XPS, MALDI TOF MS, etc.) are required for comprehensive characterization of the extracts, and for determination of the functional groups and monomers. Nevertheless, functional similarities with sodium alginate are found to be promising in terms of projecting the possible technical uses of those AGS-biopolymers. In particular, the hydrogel-forming capacity of the AGS-exoPS as presented in this study, imply potential of those waste-derived biopolymers to be used in several industrial sectors similar to the use of alginate in, e.g., textile printing, paper coating, etc. However, implementation might be limited in sectors related to direct human contact/consumption, like in production of thickeners and gelation agents in food industry, drug-delivery systems in medical applications, etc., requiring highly purified extracts [30]. Still, AGS-extracts have already been tested in some industrial applications: AGS-derived ALE was used as surface-coating agent providing water-resistance to coated papers [31]. Also, after commercially available Na-alginate was tested as a bio-polymer for curing cement-based materials [32], AGS-derived biopolymers have been commercialized as a product for the construction engineering market, offering improvement for curing of cement (http://www.ngcm.nl/curing-compound.html). Those industrial applications of AGS-exoPS point to the potential of making further use of the "wastes" from BioWWTPs by material recovery, harvesting added-value bio-products, and decreasing the amount of "waste" to be handled.

3.3.2. PHA of AGS

Biomass samples collected from the AGS system fed with raw wastewater (R1) during the period corresponding to a high organic loading rate (OLR) exhibited strong PHB-positive results (blue–black colored cells) and visually confirmed the PHB-accumulation capacity of the granular biomass. As presented in Fig. 5, individual cells, as well as cell clusters, exhibiting strong PHB(+) results were detected in appreciable amounts in all samples. In addition to individual PHB(+) cells scattered in the samples, distinctively compact clusters of PHB-accumulating organisms were also detected at the inner parts of the flocks (Fig. 5, second row) and/or at the depths of the smashed granules closer to the granule core (Fig. 5, third row).

Synthesis of PHAs was reported under deficient operation conditions such as under deficiency of oxygen, nitrogen, and phosphorus. Recently, PHA accumulation in aerobic granules was studied with synthetic wastewater (with a sole carbon source such as acetate or ethanol) under fully aerobic conditions, and the PHA contents were in the range of 18–44 % biomass (w/w) [33–36]. Li et al. [37] reported that improving the concentration of sludge, promoting the production of EPS, and decreasing the sludge floc size were effective approaches for further accumulation of the PHAs. The PHA contents in our AGS on Day 436 and Day 449 (same samples with PHB-staining) were found to be 10.8 and 9.3 %, respectively. Therefore, the relatively low PHA content in our study compared with literature should be evaluated based on real wastewater (complex carbon sources) and anaerobic/anoxic and aerobic operation conditions.

The investigated mixed liquor samples were collected from the system toward the end of the aerobic period, prior to settling and withdrawal. Accordingly, detection of PHB-accumulating organisms at significant levels in those samples not only confirmed the presence and function of those organisms but also indicated that they did not exhaust their PHB-pools by the end of the applied aerobic phase. Partial consumption of the intracellular PHA reserves under aerobic conditions

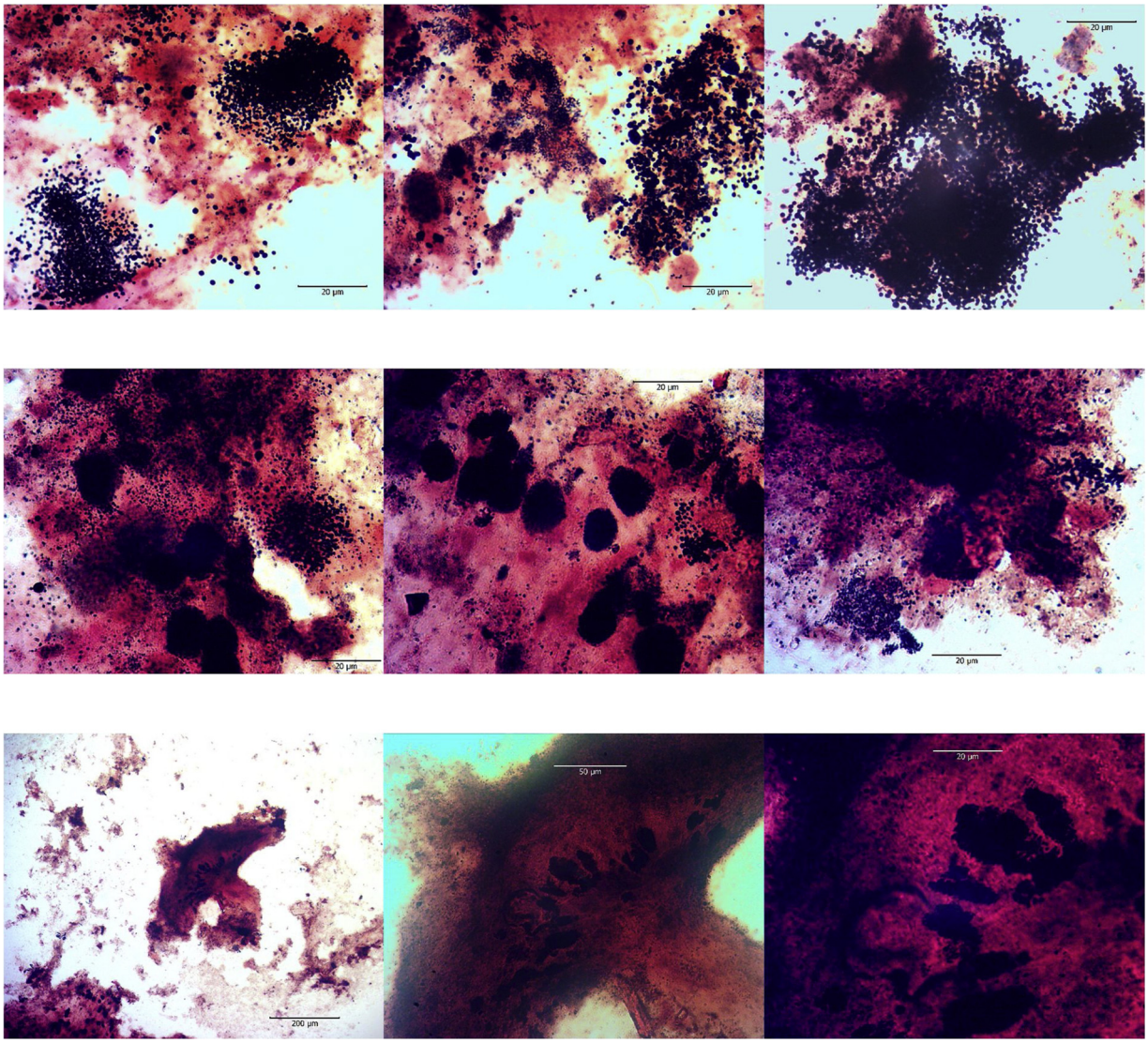


Fig. 5. PHB-staining results for the sample collected from R1 (treating raw wastewater) on Day 429 (first row) and Day 449 (second and third rows): blue–black color corresponding to PHB(+) response and pink color corresponding to PHB(−) response. First and second rows: mixed liquor samples with all scale bars showing 20 µm. Third row: staining results of a smashed granule in increasing magnification with scale bars corresponding to 200, 50, 20 µm, respectively from left to right.

might limit the subsequent anaerobic uptake of the external carbon source. In their study, to investigate the eco-physiological traits of putative GAOs, i.e., *Defluviicoccus spp*., present in relatively high levels in full-scale EBPR systems, Burow et al. [38] applied FISH-MAR and post-FISH chemical staining (for PHA and poly-P) and determined that the anaerobic-aerobic organic matter cycling behavior of the Cluster 2 *Defluviicoccus* and absence of poly-P accumulation in those organisms were in agreement with the GAO physiology. The researchers also concluded that when those organisms saturated their PHA storage capacity, they gradually lost their ability to take up the external carbon source. As described above, the biomass samples investigated in the current study had appreciable amounts of PHB-accumulating organisms which did not exhaust their PHB-reserves by the end of aeration. This result, in combination with the high OLR applied during the corresponding operational period, might explain the relatively lower anaerobic COD removal rates (30–40 %) observed during that period in R1.

The glycogen-accumulating organism (GAO) '*Candidatus Competibacter*' uses aerobically stored glycogen to enable anaerobic carbon uptake, which is subsequently stored as PHAs [39]. The microbial community analysis of the AGS evaluated in this current study showed that Uncultured *Candidatus Competibacter* sp. were the most abundant species in R1 (35 %) and R2 (8.7 %) because the OLR in R1 (3.3 ± 0.3 kgCOD.m^{-3}.day^{-1}) was higher than that in R2 (2.2 ± 0.6 kgCOD.m^{-3}.day^{-1}) during the stable period. Additionally, *Competibacteraceae* species were also the second abundant species in R1 (7.7 %) (Table S3). The ability to anaerobically store external carbon sources as PHA is the key to the competitiveness of *Competibacteraceae* under dynamic EBPR conditions [40]. The high OLR up to 3.3 kgCOD.m^{-3}.day^{-1} facilitated enrichment of those GAOs, especially in R1, and also provided an advantage to those over the EBPR-governing PAOs [14]. Combined evaluation of the results indicating COD removal under anaerobic conditions (although at lower levels), microbial community analysis showing the abundance of GAOs, PHB-staining results displaying the presence of significant amounts of PHB-accumulating organisms even by the end of aeration, and the PHA content of the AGS suggested that the AGS system might serve as a source for PHA recovery.

4. Conclusions

The study presents a novel resource recovery system based on zero-waste discharge. The system consisted of an AGS reactor and an

external MR from which irrigation water and biopolymers can be recovered. The study highlighted that boron concentrations should be carefully checked because boron in treated wastewater of AGS-MR systems was higher than that in the irrigation water standards. Structural EPS was recovered from the AGS of the integrated system. They showed the capacity to form hydrogels, thus exhibiting a promising potential for several technical uses. Operating the AGS reactor under high OLR conditions resulted in enrichment of the GAOs, which are known as mostly PHA accumulating bacteria, microbiological observations, and the PHA content of the AGS confirmed PHB-accumulation capacity of the AGS. Therefore, the treatment system was considered as a potential resource for PHA recovery. Because the membrane concentrate contained a high amount of biomass patches, the possibility of recovering similar biopolymers from the membrane concentrate needs to be explored further to further contribute to the "circular economy" of the integrated system.

Declaration of Competing Interest

Hereby, the authors declare that the content of this article is subject to no conflict of interest.

Acknowledgment

This work was funded by The Scientific and Technological Research Council of Turkey, TUBITAK (Project No: 111Y036). It has been patented by Turkish Patent and Trademark Office (Patent No:TR 2015 16527 B).

Appendix A. Supplementary data

Supplementary material related to this article can be found, in the online version, at doi:https://doi.org/10.1016/j.jwpe.2020.101148.

References

[1] A.J. Ansaria, F.I. Haia, W.E. Priceb, J.E. Drewesc, L.D. Nghiema, Forward osmosis as a platform for resource recovery from municipal wastewater - A critical assessment of the literature, J. Membr. Sci. 529 (2017) 195–206.
[2] M.E. Mattson, Significant developments in membrane desalination-1979, Desalination 28 (3) (1979) 207–223.
[3] B. van der Bruggen, L. Braeken, The challenge of zero discharge: from water balance to regeneration, Desalination 188 (2006) 177–183.
[4] J.S. Guest, et al., A new planning and design paradigm to achieve sustainable resource recovery from wastewater, Environ. Sci. Technol. 43 (2009) 6126–6130.
[5] X. Hao, C. Wang, M.C.M. van Loosdrecht, Y. Hu, Looking beyond struvite for P-recovery, Environ. Sci. Technol. 47 (10) (2013) 4965–4966.
[6] Y. Lin, M. de Kreuk, M.C. van Loosdrecht, A. Adin, Characterization of alginate-like exopolysaccharides isolated from aerobic granular sludge in pilot-plant, Water Res. 44 (11) (2010) 3355–3364.
[7] P. Westerhoff, S. Lee, Y. Yang, G.W. Gordon, K. Hristovski, R.U. Halden, P. Herckes, Characterization, recovery opportunities, and valuation of metals in municipal sludges from U.S. wastewater treatment plants nationwide, Environ. Sci. Technol. 49 (16) (2015) 9479–9488.
[8] C.J. Ruiken, G. Breuer, E. Klaversma, T. Santiago, M.C. van Loosdrecht, Sieving wastewater - cellulose recovery, economic and energy evaluation, Water Res. 47 (1) (2013) 43–48.
[9] L.M.M. de Bruin, M. de Kreuk, H.F.R. van der Roest, C. Uijterlinde, M.C.M. van Loosdrecht, Aerobic granular sludge technology: an alternative to activated sludge? Water Sci. Technol. 49 (11–12) (2004) 1–7.
[10] M. Pronk, T.R. Neu, M.C.M. van Loosdrecht, Y.M. Lin, The acid soluble extracellular polymeric substance of aerobic granular sludge dominated by *Defluviicoccus* sp, Water Res. 122 (2017) 148–158.
[11] D.R. de Graaff, S. Felz, T.R. Neu, M. Pronk, M.C.M. van Loosdrecht, Y. Lin, Sialic acids in the extracellular polymeric substances of seawater-adapted aerobic granular sludge, Water Res. 155 (2019) 343–351.
[12] S. Felz, P. Vermeulen, M.C.M. van Loosdrecht, Y.M. Lin, Chemical characterization methods for the analysis of structural extracellular polymeric substances (EPS), Water Res. 157 (2019) 201–208.
[13] T. Seviour, et al., Extracellular polymeric substances of biofilms: suffering from an identity crisis, Water Res. 151 (2019) 1–7.
[14] E. Cetin, E. Karakas, E. Dulekgurgen, S. Ovez, M. Kolukirik, G. Yilmaz, Effects of high-concentration influent suspended solids on aerobic granulation in pilot-scale sequencing batch reactors treating real domestic wastewater, Water Res. 131 (2018) 74–89.
[15] APHA, AWWA, WEF, Standard Methods for the Examination of Water and Wastewater, American Public Health Association, Washington DC, USA, 1995 ISBN 0-87553-223-3.
[16] B. Frølund, R. Palmgren, K. Keiding, P.H. Nielsen, Extraction of extracellular polymers from activated sludge using a cation exchange resin, Water Res. 30 (8) (1996) 1749–1758.
[17] M. Kumar, A. Gupta, I.S. Thakur, Carbon dioxide sequestration by chemolithotrophic oleaginous bacteria for production and optimization of polyhydroxyalkanoate, Bioresour. Technol. (2016) 213.
[18] D. Jenkins, M.G. Richard, G.T. Daigger, Manual on the Causes and Control of Activated Sludge Bulking and Foaming, 2nd ed., Lewis Publishers Inc., Michigan, USA, 1993, p. 25 ISBN 0-87371-873-9.
[19] A. Klindworth, E. Pruesse, T. Schweer, J. Peplles, C. Quast, et al., Evaluation of general 16S ribosomal RNA gene PCR primers for classical and next-generation sequencing-based diversity studies, Nucleic Acids Res. 41 (1) (2013).
[20] T.Z. de Santis, P. Hugenholtz, N. Larsen, M. Rojas, E.L. Brodie, K. Keller, T. Huber, D. Dalevi, P. Hu, G.L. Andersen, Greengenes, a chimera-checked 16S rRNA gene database and workbench compatible with ARB, Appl. Environ. Microbiol. 72 (7) (2006) 5069–5072.
[21] R. Pishgar, J.A. Dominic, Z. Sheng, J.H. Tay, Influence of operation mode and wastewater strength on aerobic granulation at pilot scale: startup period, granular sludge characteristics, and effluent quality, Water Res. 160 (2019) 81–96.
[22] S.B. Sam, E. Dulekgurgen, Characterization of exopolysaccharides from floccular and aerobic granular activated sludge as alginate-like-exoPS, Desalin. Water Treat. 57 (6) (2016) 2534–2545.
[23] S. Felz, S. Al-Zuhairy, O.A. Aarstad, M.C. van Loosdrecht, Y.M. Lin, Extraction of structural extracellular polymeric substances from aerobic granular sludge, J. Vis. Exp. 115 (2016) e54534, , https://doi.org/10.3791/54534.
[24] S.-J. Yuan, M. Sun, G.-P. Sheng, Y. Li, W.-W. Li, R.-S. Yao, H.-Q. Yu, Identification of key constituents and structure of the extracellular polymeric substances excreted by *Bacillus megaterium* TF10 for their flocculation capacity, Environ. Sci. Technol. 45 (2011) 1152–1157.
[25] A.R. Badireddy, S. Chellam, P.L. Gassman, M.H. Engelhard, A.S. Lea, K.M. Rosso, Role of extracellular polymeric substances in bioflocculation of activated sludge microorganisms under glucose-controlled conditions, Water Res. 44 (2010) 4505–4516.
[26] D. Leal, B. Matsuhiro, M. Rossi, F. Caruso, FT-IR spectra of alginic acid block fractions in three species of brown seaweeds, Carbohydr. Res. 343 (2008) 308–316.
[27] B.-B. Wang, X.-T. Liu, J.-M. Chen, D.-C. Peng, F. He, Composition and functional group characterization of extracellular polymeric substances (EPS) in activated sludge: the impacts of polymerization degree of proteinaceous substrates, Water Res. 129 (2018) 133–142.
[28] C. Yin, F. Meng, G.-H. Chen, Spectroscopic characterization of extracellular polymeric substances from a mixed culture dominated by ammonia-oxidizing bacteria, Water Res. 68 (2015) 740–749.
[29] S. Felz, T.R. Neu, M.C.M. van Loosdrecht, Y. Lin, Aerobic granular sludge contains Hyaluronic acid-like and sulfated glycosaminoglycans-like polymers, Water Res. 169 (2020) 115291.
[30] G.A. Paredes-Juarez, M. Spasojevic, M.M. Faas, P. de Vos, Immunological and technical considerations in application of alginate-based microencapsulation systems, Front. Bioeng. Biotechnol. 2 (2014) 1–15.
[31] Y.M. Lin, K.G.J. Nierop, E. Girbal-Neuhauser, M. Adriaanse, M.C.M. van Loosdrecht, Alginate-like exopolysaccharides characterization and utilization, Proc. IWA Conf.-The Perfect Slime: Nature, Properties, Regulation and Dynamics of EPS, 10-12 Sept 2014, Essen-Germany, 2014, p. 75.
[32] J. Zlopasa, E.A.B. Koenders, S.J. Picken, Using bio-based polymers for curing cement-based materials, Proc. Int. Conf. on Aging of Materials and Structures, 26-28 May 2014, Delft-The Netherlands, 2014, pp. 220–226.
[33] L. Qin, Y. Liu, J.H. Tay, Denitrification on poly-*β-hydroxybutyrate* in microbial granular sludge sequencing batch reactor, Water Res. 39 (2005) 1503–1510.
[34] F. Fang, X.W. Liu, J. Xu, H.Q. Yu, Y.M. Li, Formation of aerobic granules and their PHB production at various substrate and ammonium concentrations, Bioresour. Technol. 100 (2009) 59–63.
[35] J. Wang, W.W. Li, Z.B. Yue, H.Q. Yu, Cultivation of aerobic granules for polyhydroxybutyrate production from wastewater, Bioresour. Technol. 159 (2014) 442–445.
[36] A. Wosman, Y. Lu, S. Sun, X. Liu, C. Wan, Y. Zhang, D.J. Lee, J.H. Tay, Effect of operational strategies on activated sludge's acclimation to phenol, subsequent aerobic granulation, and accumulation of polyhydoxyalkanoates, J. Hazard. Mater. 317 (2016) 221–228.
[37] H. Li, J. Zhang, L. Shen, Z. Chen, Y. Zhang, C. Zhang, Q. Li, Y. Wang, Production of polyhydroxyalkanoates by activated sludge: correlation with extracellular polymeric substances and characteristics of activated sludge, Chem. Eng. J. 361 (2019) 219–226.
[38] L.C. Burow, Y. Kong, J.L. Nielsen, L.L. Blackall, P.H. Nielsen, Abundance and ecophysiology of Defluviicoccus spp., glycogen-accumulating organisms in full-scale wastewater treatment processes, Microbiology 153 (2007) 178–185.
[39] W.-T. Liu, T. Mino, K. Nakamura, T. Matsuo, Role of glycogen in acetate uptake and polyhydroxyalkanoate synthesis in anaerobic-aerobic activated sludge with minimized polyphosphate content, J. Ferm. Bioeng. 77 (1994) 535–540.
[40] S.J. McIlroy, M. Albertsen, E.K. Andresen, A.M. Saunders, R. Kristiansen, M. Stokholm-Bjerregaard, K.L. Nielsen, P.H. Nielsen, '*Candidatus* Competibacter'-lineage genomes retrieved from metagenomes reveal functional metabolic diversity, ISME J. 8 (2014) 613–624.
[41] Turkish Republic Ministry of Environment and Urban Planning, Water Pollution Control Regulation Directive for Wastewater Treatment Plants, Official Gazette Dated March 20, (2010) and issued 27527.